DISCRETE AND CONTINUOUS
DYNAMICAL SYSTEMS
Volume **33**, Number **9**, September **2013**

doi:10.3934/dcds.2013.33.xx

pp. X–XX

ARCHIMEDEAN ICE

Kari Eloranta

Department of Mathematics, Aalto University
P. O. Box 11100, FI-00076 Aalto, Finland

ABSTRACT. The striking boundary dependency, the Arctic Circle Phenomenon, exhibited in the Ice model on the square lattice extends to other planar set-ups. This can be shown using a dynamical formulation which we present for the Archimedean lattices. Critical connectivity results guarantee that the Ice configurations can be generated using the simplest and most efficient local actions. Height functions are utilized throughout the analysis. On a hexagon with suitable boundary height the cellular automaton dynamics generates highly nontrivial Ice equilibria in the triangular and Kagomé cases. On the remaining Archimedean lattice for which the Ice model can be defined, the 3.4.6.4. lattice, the long range behavior is shown to be completely different due to strictly positive entropy for all boundary conditions.

1. Introduction. Although the best known version of the Ice model is that defined on the square lattice ([1], [9]), the construction is quite natural on a number of other lattices as well. Here we investigate using dynamical methods the basic properties of the bounded version of the model on the other Archimedean lattices: triangular, Kagomé and 3.4.6.4. lattices. The investigation serves two purposes. Firstly it complements the various studies of the infinite unbounded models and answers the question on the influence of the boundary posed already by Kasteleyn ([7]). Secondly we hope to contribute whatever is possible to the unification of the theories of lattice statistical mechanics, higher dimensional symbolic dynamics and tilings that has been worked on for some time now (starting from ([3], [11], for later developments see e.g. [8], for Ice e.g. [2]).

Our results show that 18/20/36-vertex models (Ice on Kagomé, triangular and 3.4.6.4. lattices respectively) can to a certain extent be analyzed with similar means than the square lattice one (the Six-vertex model). They have analogous cycle structure which facilitates the configuration computation with simple and efficient cellular automata algorithms. Height works in the same way in these models and the boundary effects it forces are qualitatively similar – up to a point. There can be a sharp a demarcation of temperate and frozen subdomains akin to the Arctic Circle Phenomenon in Dominoes/Dimer model originally discovered by Propp et. al., see [6]. In the triangular and Kagomé Ice the demarcation can be observed but just as in the context of e.g. the Hard square/hexagon model ([1]) there is a surprising lattice dependency already within the set of the four possible Archimedean lattices. Indeed the influence of the underlying lattice is even more pronounced here: Ice on 3.4.6.4. lattice is in terms of long range order a qualitatively different model from

2010 Mathematics Subject Classification. Primary: 37A60, 82C20; Secondary: 82C27.

Key words and phrases. Ice model, vertex rule, Archimedean lattice, cellular automaton, measure of maximal entropy, spatial phase transition.

This research was partially supported by Finnish Academy of Science.

The paper was reported at the satellite conference on "Various Aspects of Dynamical Systems," following ICM 2010.

the three other versions of Ice. It shows strong uniformity in the configurations independent of the boundary condition.

Whenever analyzing the bounded 6/18/20/36-vertex models, similarities admitting, we refer to the results already established for the Six-vertex model ([4]) and concentrate here on the novel features. We make however an effort to make this paper self-contained so that the reader can grasp the main ideas and all the new results from here.

1.1. Set-up. In the **vertex-models** of the Statistical Mechanics instead of spin variables one deals with arrow orientations between nearest neighbor lattice sites. The global ensemble of the orientations defines the configuration.

Definition 1.1. A **vertex configuration** is the arrangement of arrows arriving to and departing from a lattice point. It is **legal** for the **ice rule** if there is the same number of incoming and outgoing arrows at that lattice point. If there is a legal vertex configuration at every vertex of the lattice the arrow configuration is legal for the **Ice model**.

In the square lattice case there are six such vertex configurations, hence the Ice model on that lattice is also called the **Six-vertex model**. The term "Ice" stems from the physical interpretation for this model ([9]). Although this physical interpretation does not carry over to other lattices, for simplicity we call those rules **ice-type**. For the purposes of this paper we only consider Ice on planar lattices.

A rule of this kind obviously requires even vertex degree. Among the three regular planar lattices – the square, triangular and hexagonal lattices – Ice model can be defined on the first two. The next simplest planar lattices are the **Archimedean** or **uniform lattices**. They are defined via tilings: their bonds correspond to the tile edges of such tilings by regular polygons which are up to rotation identical at each vertex. There are 21 ways of tiling a vertex neighborhood with regular polygons. 11 of these arrangements extend to the plane - these are the Archimedean tilings (complete list [5]). Among these we have four lattices with even vertex degree: square, triangular, Kagomé and 3.4.6.4. lattices (the code number $n_1.n_2.n_3.n_4$. lists the n-gons that one sees turning once around a vertex). In physical terms these are the simplest discrete planar structures that accommodate the dipole/incompressibility restriction of the ice-type.

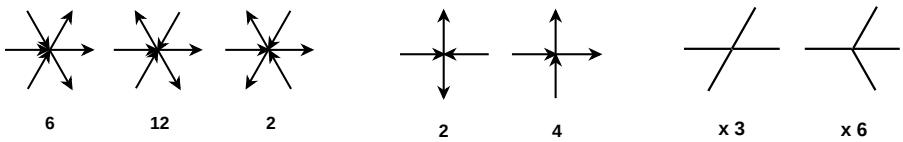

Figure 1a, b, c. Vertex configurations: arrow arrangements and multiplicities.

The available vertex configurations are illustrated in Figure 1. Triangular lattice is on the left with multiplicities accounting rotations and reflections listed below. In the center we have the analogous arrangements for the square lattice. The multiplicities for Kagomé and 3.4.6.4. are obtained from those of the square lattice vertex configurations by multiplying them with the numbers on the right, below (the numbers of possible orientations of the middle arrangements in these lattices). Adding the numbers up we could call these 20/6/18/36-vertex models (for triangular, square, Kagomé and 3.4.6.4. lattices respectively) but for simplicity we just

call them ice models on the appropriate lattice.

The Square ice on a bounded domain was considered in an earlier paper ([4]). Here we study the other three models on a hexagonal domain. A N**-hexagon** in the case of the triangular lattice is a domain which is oriented along the lattice axes with N boundary arrows along each edge, N even. Or equivalently we can require that along each edge there are $N/2$ lattice sites with all six arrows attached to them. Figure 2a. illustrates the area around leftmost corner of such hexagon (the boundary will have six-fold symmetry). The **boundary arrows**, $6N-6$ in total, are rendered bold. They will be fixed and the main problem will be determining when and how the interior arrows (lighter) can be arranged into a legal configuration.

The other simple domain shapes on the lattice, a unilateral triangle and a rhombus turn out to be somewhat restrictive due to the acute corners. On the hexagonal domain we will be able to illustrate both "ordered/frozen" and "disordered/temperate" configurations and their coexistence as in a diamond in the square lattice case in our earlier study.

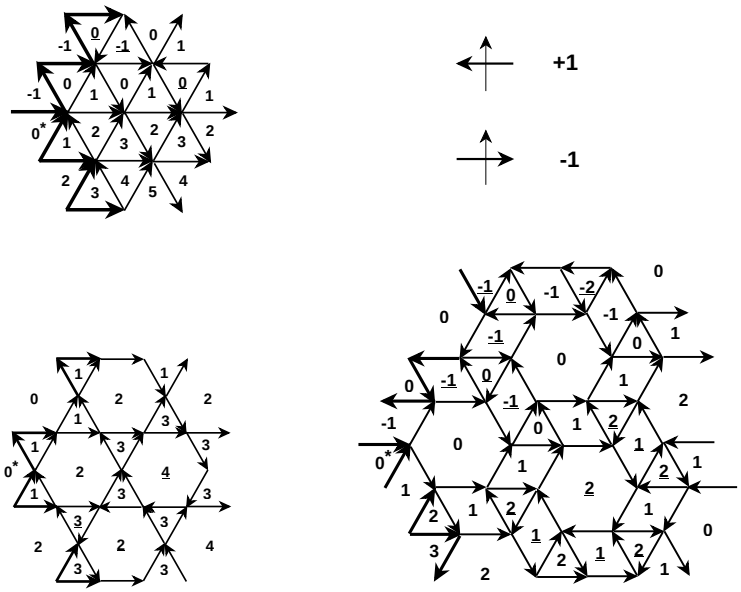

Figure 2a, b (top), c, d (bottom). The crossing rule and configurations with heights.

The dual lattice of the triangular lattice is the hexagonal lattice. Every lattice site is the center of a minimal (unit) hexagon the boundary of which we should think of having a clockwise orientation. By the ice rule the total **flux** across this boundary is zero (in going arrow counts $+1$, outgoing -1). Consider the maximal dual lattice loop on the domain, **the boundary loop** (the dual lattice edges of this loop still cross arrows in the N-hexagon). It is the sum of all the directed unit hexagons in the dual lattice inside the domain. Hence if the configuration inside the domain is legal then the flux across the boundary loop vanishes.

In the Kagomé-lattice N-hexagon has N lattice sites and $N/2$-arrows along each edge. Figure 2c. illustrates the leftmost corner of such hexagon. The bold arrows

are again the fixed boundary arrows. Because of the ice-rule the flux around each lattice point vanishes. Therefore a legal fill-in of a hexagon will have zero boundary flux. Same principles extend to the 3.4.6.4. lattice case.

Let C be the set of legal ice configurations on a given triangular lattice hexagon and let D, the **dual cover**, denote the finite subset of the hexagonal lattice that has the property that an edge connecting a nearest neighbor pair of vertices from D crosses an arrow $c \in C$.

The **height**, $f : C \times D \to Z$, is an extremely useful function in analyzing ice-type models. Its increments on D are defined by the crossing rule in Figure 2b. The light arrow indicates the edge on the dual lattice that we move along and the bold marks the configuration arrow. The rules apply in all possible rotations. Note that height around a closed loop in D vanishes (since this is the same as computing the flux across that loop). Hence f is independent of the path along which it was computed. To be unique it needs to be specified at one **base point** which we choose to be the leftmost dual lattice point (starred). In Figure 2a. we have indicated the heights with the choice that at the base point height vanishes.

The dual of the Kagomé/3.4.6.4. lattice is the rhombus-lattice [3.6.3.6]/[3.4.6.4] respectively. The definition of height on them is as above and we have indicated the values in Figure 2c. and 2d (The numbers in square brackets refer to Laves tilings, see [5]. Note that 3.4.6.4. being rendered here so that squares turn into lozenges does not in any way affect arguments since the neighborhood topology remains intact).

Height is a Lipschitz-function with constant 2: $|f(c, d_1) - f(c, d_2)| \leq 2m(d_1, d_2)$, were m is a metric on dual cover of the unit lattice. A rather natural choice is the Manhattan metric i.e. minimal hop count between $d_i \in D$ scaled with the lattice unit. Height is a rather well behaved function and in here as in the Domino context one can often approximate it linearly.

The three cases when height is monotone increasing/decreasing or alternates along a path in the dual lattice will be important in later considerations. As the boundary specification will be critical we have chosen to illustrate this on the boundaries in Figure 2. The boundary arrows in the lower halves of the samples are such that the height decreases monotonically as we trace the boundary clockwise. The upper half of the boundary illustrate the alternating case.

2. Connectivity. Consider a legal triangular, Kagomé or 3.4.6.4. ice configuration. Suppose that we can find a closed unidirectional path of configuration arrows in it (or a path from infinity to infinity). Reversing this directed cycle i.e. flipping every arrow on the cycle results in an other legal configuration since the rule at each vertex is respected. Existence of an unidirectional cycle is therefore related to the non-uniqueness of the fill-in: a boundary arrangement of arrows that allows a fill-in which has an off-boundary unidirectional cycle allows in fact multiple fill-ins.

Definition 2.1. Call the smallest lattice triangle a **1-triangle**. The orientation $\triangle$ is **even** and $\triangledown$ is **odd**. On the Kagomé lattice we also have a minimal hexagon, a **1-hexagon** and on the 3.4.6.4. lattice we additionally have left-leaning, right-leaning and straight standing **1-lozenges**. If these directed **1-polygons** are unidirectional we call them **1-cycles** and their reversals **local moves**.

In Figure 2a, c and d. the sample configurations contain 1-cycles indicated by underlined height. By utilizing flux as in [4] one can in fact show that

Proposition 2.2. *A unidirectional cycle always encloses a 1-cycle.*

We say that a cycle is **off-boundary** if it does not contain any of the (fixed) boundary arrows. Define a bounded **frozen** configuration to be one without off-boundary 1-cycles. Its opposite is the **temperate** configuration which we define as one having a directed cycle boundary.

Related to the 1-cycles there is a simple but useful notion which we will need in the proof below. In Figure 3a, b. the infinite wedges C_i rooted at the vertices of the 1-cycles are **contact sectors**. For the triangle oriented upside down we reflect the wedges and for 1-hexagon we have for clarity indicated only the odd sectors.

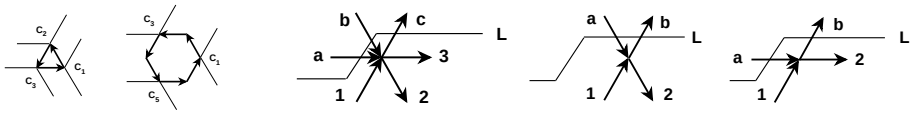

Figure 3a, b. Contact sectors. **c, d, e.** Vertex configuration mismatch.

Theorem 2.3.1. *On triangular and Kagomé lattices the set of Ice configurations with common boundary arrows on a N-hexagon is connected under 1-cycle reversals i.e. two such configurations can be transformed to each other with a finite sequence of 1-cycle reversals.*

Proof. The argument uses a "lexicographic sweep" refined from [4]. When during the sweep we arrive to a lattice point l where there is the next mismatch between the two configurations under comparison, the situation in triangular lattice looks like in Figure 3c. L denotes the "front" above which all vertex configurations in the two configurations match. In the Kagomé case we may encounter three different arrangements, two of which are in Figures 3d, e. (the third is like the rightmost, but rotated 60 degrees clockwise).

Consider the case of triangular lattice. The three arrows $a-c$ cannot all be in or all out since in that case there cannot be a mismatch. So among arrows $1-3$ there is a 2-1 or 1-2 split between ingoing and outgoing arrows. Hence we can always find among them a pair ($(1,2)$, $(1,3)$ or $(2,3)$), same 2-path on both configurations, so that the arrows in them are unidirectional but oriented opposite in the two paths. Then tracing pairs of arrows with opposite orientations at the same location in the two configurations one then extends these 2-paths to identical off-boundary cycles with opposite orientations in the two configurations.

Pick one of the configurations e.g. the one with clockwise oriented cycle, O_1. By Proposition 2.2. inside it there is at least one 1-cycle of some type. Denote their collection by $\{C_i\}$. Choose two of its contact sectors in such a way that they do not overlap and do not contain the point of mismatch l. It is then possible to find two directed paths, one in each of the contact sectors, which connect the 1-cycle to O_1 (as in Theorem 2.3. of [4]). Moreover the orientations of these paths are such that a new clockwise directed cycle is formed that passes through l, along the edge of the 1-cycle and is contained in the domain bounded by O_1. This construction is done to all of the 1-cycles inside O_1. Finally define the natural minimal directed cycle along these new cycles inside O_1 and call it $\tilde{O}_1$.

Now some the 1-cycles inside O_1 are on the boundary of the $\tilde{O}_1$ and none are strictly in its interior. By reversing these cycles if necessary we obtain a new directed cycle O_2 with the property that all of the 1-cycles $\{C_i\}$ are left outside it. Moreover

O_2 encloses a strictly smaller area than O_1, all inside it.

Applying the argument above to O_2, O_3 and so on finally forces a 1-cycle that has l as its vertex. Hence we correct a mismatch at l. Note that if the path O_1 involved the pair $(1,3)$ we need a second application of this argument, now to a loop through $(1,2)$ or $(2,3)$, whichever pair is still mismatched in the two configurations. After this all arrows at l match and the front L moves to the next lexicographic location to check for a mismatch.

For the Kagomé lattice one pass of the argument above suffices. Whether the 1-cycle is a 1-triangle or 1-hexagon affects only the choice of the contact sectors. □

We present the argument above since it extends the one in [4] for the square lattice case and also since it seems to be the most transparent way to argue the result. The argument is also quite general holding for other domains and 3.4.6.4. lattice as well. Since the contact sectors do not work so easily for the latter we now sketch an alternative proof (for the most general argument see [10]).

For all our four lattices the height function introduces a partial order in the set of configurations with common boundary configuration: $c_1 \succeq c_2$, if $f(c_1, d) \geq f(c_2, d)$, $\forall d \in D$. The local minima of the height surface are simply the center points of counterclockwise oriented 1-cycles. If these are off-boundary one can reverse them and reach strictly higher height. After a finite number of steps one arrives at the maximal element $\overline{c}$: $f(\overline{c}, d) \geq f(c, d)$, $\forall d$, any c with the same boundary configuration. The maximal element has by definition no off-boundary counterclockwise oriented 1-cycles. Through this (or the minimal element) one connects all the configurations with a finite sequence of local moves. Hence

Theorem 2.3.2. *The set of 3.4.6.4. ice configurations with common boundary arrows on a N-hexagon is connected under 1-cycle reversals.*

Through counterexamples we now see that no smaller set of local moves suffices. Suppose that we have a configuration on the triangular lattice where each of the lattice arrows is directed either toward 1, 3 or 5 o'clock. Then reverse all the arrows on one of the 1 o'clock and 5 o'clock lattice lines. Cut a N-hexagon out from this so that the intersection of these lattice lines is at the center. The patch that we see at the center of the hexagon looks like Figure 4a.

Reversing the 1-triangle at C will obviously not affect the boundary arrows i.e. we get another configuration, call it $\tilde{H}$, compatible with the boundary configuration. If we are subsequently only allowed to act with $\triangle$-reversals there will be only two such triangles to work on, the one at T in $\tilde{H}$ and the one below C. But it is easy to see that reversing these and any other directed $\triangle$-cycles will never yield a directed cycle outside the two acute wedges defined by the bold lines. Hence two sides of C will never be returned to their original orientation.

In the case of Kagomé lattice we generate a configuration as above, this time from arrow lines pointing toward 3, 7 and 11 o'clock. This configuration has has the property that all 1-triangles are directed (see Figure 4b.). If we reverse any one of them, say C, the new configuration is compatible with the boundary but still has no directed 1-hexagons. Notice that even if only the reversal of $\bigtriangledown$ is forbidden we are still stuck. Reversing C cannot be undone with $\triangle$-actions and all the 1-hexagons will still remain undirected.

If the configuration is generated in an alternating fashion from arrow lines to directions 1 and 7, 3 and 9 and 5 and 11 o'clock we can see in it a patch like Figure

4c. If we reverse the 1-hexagon, the 1-triangles around it will become directed but the David's star is isolated from the 1-cycle reversals outside it, so its original orientations cannot be returned.

For the 3.4.6.4. lattice consider the arrangement on the right, Figure 4d. This hexagon clearly extends to a unique global configuration. Suppose we reverse the even triangle marked with C and then ban subsequent even 1-triangle reversals. It is easy to see that the right-leaning lozenges can never be reversed in this configuration. Hence return to the original configuration is impossible. Similarly if after this move we reverse the left-leaning lozenge at L and then ban left-leaning lozenge moves, the original configuration cannot be recaptured with the remaining moves.

Finally if we pick a configuration with only 1-cycles, flip one of the 1-hexagons and then forbid 1-hexagon moves, no neighboring lozenges can be reversed and the original configuration cannot be recaptured. All together we have

Proposition 2.4. *The connectivity results fail if not all 2/3/6 types of local moves are available for triangular/Kagomé/3.4.6.4. lattices respectively.*

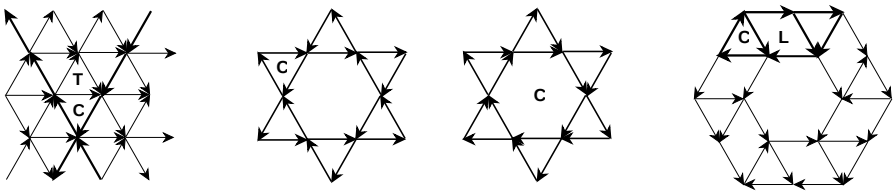

Figure 4a, b, c, d. Restricted actions.

3. Ice through dynamics. From the practical point of view the most significant consequence of Theorems 2.3.x. is that they facilitate the generation of the configurations with a given boundary configuration. We now indicate how this is done. The aim here is simply to get an algorithm to study the model, not run time considerations.

The ensemble of arrows on the triangular lattice can be viewed as an array of either just even or just odd 1-triangles with oriented sides. Call their restrictions to the N-hexagon L_e and L_o respectively. This is not a partition since each off-boundary arrow is in one even and in one odd triangle.

On the triangle arrays we define two local update rules. If an off-boundary even/odd 1-cycle is encountered, it is reversed independently with probability 1/2 and also its odd/even nearest neighbor 1-triangles are updated accordingly. These rules give global random maps F_e and F_o which check 1-cycles on L_e and L_o respectively and independently update the arrow configuration on both. They define a **probabilistic cellular automaton (pca)** action on the configurations.

On the Kagomé lattice we additionally define a local rule reversing an unidirectional off-boundary 1-hexagon with probability 1/2 and updating the six neighboring 1-triangles. Call the global map of independent flips F_h. The updating sequence $\{F_e, F_o, F_h\}$ defines a pca cycle. In the 3.4.6.4. lattice case we have to perform the lozenge flips as well. Let F_l F_r and F_s denote the probability 1/2 flips of the left leaning, right leaning and straight standing off-boundary lozenges respectively. The updating sequence $\{F_e, F_o, F_s, F_l, F_r, F_h\}$ has been used in the generation of the configurations of this ice model.

For a given boundary condition the set of legal fill-ins and the local moves constitutes a finite Markov Chain. Suppose (as above) that all possible transitions have positive probability. Theorems 2.3.x. imply the irreducibility of this chain. Because of the positive transition probabilities the chain is also aperiodic. Hence the chain is ergodic: given any initial configuration the pcas above will eventually generate any configuration compatible with the boundary configuration of the initial one and weight them uniformly (according to the measure of maximal entropy) ([12]). The choice of probability $1/2$ for the flip is for maximal speed. Note that in each of the lattices the densities of the 1-n-gons of all types are the same (in the set of all 1-polygons). Hence in the update schemes above all local moves are weighted equally. We do not know of any rigorous relaxation rate result applicable here but in all simulations it seemed exponential.

4. Boundary dependency. We now investigate the key feature of the finite versions of these lattice models – the long range boundary dependency. Among the Ice models the square lattice case has already revealed a striking phenomenon, the existence of an Arctic Circle delineating the random and ordered subdomains ([4]). Here we split the analysis for the other Archimedean lattices in two subsections since a surprising demarcation takes place. The material here contains both rigorous results and computer simulations using the principles from above.

4.1. Triangular and Kagomé cases. By the **boundary height**, f^∂, of a configuration we mean the restriction of height to the boundary of the dual cover D (see Section 1.1.): computing it we follow the boundary loop thereby only crossing boundary arrows.

If the boundary height over a segment is monotone increasing, monotone decreasing or alternating we say that the segment has **tilt** $+1, -1$ and 0 respectively. Suppose that the boundary height on each entire edge of the hexagon is either monotone increasing, decreasing or alternating. Then the **signature** of the boundary is the six-vector that we gets by recording the tilts starting from the base point and circumambulating the boundary of D clockwise.

For both triangular and Kagomé lattices the signature $(+1, +1, 0, -1, -1, 0)$ and its cyclic permutations correspond to perfectly ordered configurations. They are frozen i.e. contain no directed 1-cycles.

The signature $(0, 0, 0, 0, 0, 0)$ is the maximally disordered case and the configurations are temperate. Now the boundary arrows form unidirectional paths which are at least the length of the edge. The case where the entire boundary is a unidirectional cycle has this signature and clearly has the largest such cycle in any hexagon.

Let $A(N)$ be the number of non-boundary arrows in a N-hexagon and let $C(N)$ be the number of legal fill-ins for a given boundary condition. Then it is natural to call $h_N = \frac{1}{A(N)} \log C(N)$ the **entropy of a boundary condition.** If a configuration is given with its boundary we can also refer to this number as the **entropy of a configuration**.

Suppose that the lattice spacing is set to be $1/N$. Then the configuration is defined in a discrete subset of a unit hexagon. If a sequence of boundary heights $\{\frac{1}{N} f_N^\partial\}$ converges as $N \to \infty$ to a limiting function f^∂ we call this the **asymptotic boundary height**. As the argument and the image are scaled identically and the height is a Lipschitz-function, so is f^∂. Whenever f^∂ is differentiable, its derivative

along the boundary generalizes the notion of tilt. Finally if both f^∂ and $h = \lim_N h_N$, exist, the latter gives the asymptotic exponential size of the set of legal configurations for the corresponding asymptotic boundary height.

The frozen case corresponds to a boundary height that uniquely defines the entire height and thereby the configuration. A directed cycle boundary has asymptotically vanishing boundary height and admits maximal number of fill-ins. Between these extrema there are many possibilities. As we will see even in the relatively simple cases where the boundary tilt is piecewise constant, typical configurations can be highly non-trivial.

Proposition 4.1. *For the triangular and Kagomé lattice the entropy can attain arbitrarily small positive values in the scaling limit.*

Proof. Consider a seed configuration on the triangular lattice with initial arrow orientations as indicated in Figure 5a for a small hexagon. The construction for the Kagomé (and square) lattice is essentially the same and we omit it.

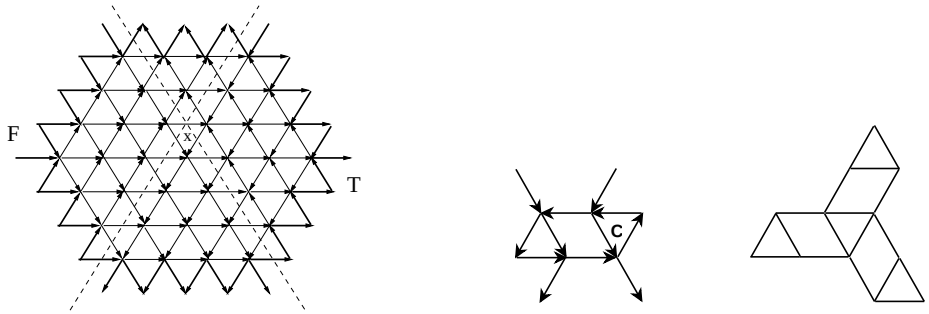

Figure 5a, b, c. Low entropy construction, forced cycle and the cycle template.

Note that in the construction along each lattice line the arrow orientation across the hexagon is constant. The dotted extra lines are defined by the locations where this orientation reverses/the boundary condition (bold arrows) changes. They intersect at x thereby dividing the domain into quadrants. The leftmost one, F, is clearly frozen; when the pca runs from this initial state the arrows within F will remain unchanged since no 1-cycles can be introduced to this subdomain. The opposite quadrant on the right, T, is initially all directed 1-cycles (both even and odd). When the pca runs these will introduce directed 1-cycles to the top and bottom quadrants as well.

Let A_T, A_F^c and A denote the number of 1-triangles in T, in the off-F area and the total number respectively. By only flipping say even unidirectional 1-triangles one immediately establishes the positive lower bound $\frac{A_T}{2A}\log 2$ for the entropy. Similarly the number $\frac{A_F^c}{A}\overline{h}$ bounds the entropy from above (free action on A_F^c). Here $\overline{h}$ is the (finite) entropy of the free infinite model.

The areas A_T, A_F^c are determined by the location of the intersection point x, which in turn is determined by the boundary condition. If x is the rightmost point of the hexagon we have a zero entropy case whereas if x is the leftmost point on the boundary we are in the maximally disordered case. The boundary height is here of piecewise constant tilt ± 1 or 0, hence the limiting boundary height exists. When the scaling step $1/N$ is fine enough we can reach arbitrarily small positive entropy value simply by forcing x far enough to the right. □

A more general statement it likely to be true. However proving it would require some detailed information on the measure of the maximal entropy which we do not currently have.

Claim 4.2. *For the triangular and Kagomé lattices the entropy as a function of the boundary height can attain any value between 0 and $\overline{h}$ in the scaling limit.*

We now present some less trivial boundary conditions that lead to a striking illustration of the long range order in the ice on triangular and Kagomé set-up.

The signature choice $(-1,+1,-1,+1,-1,+1)$ is recorded in Figure 6a., top. This height choice leads to the coexistence of frozen and temperate domains. Figure 6a. middle illustrates the even 1-cycle flip distribution on a triangular lattice 99-hexagon. Here we have recorded the site wise cumulative total of even 1-cycle reversals during the iterates $10^5 - 3 \times 10^5$ when the system was extremely close to equilibrium. Brighter cells indicate higher flip activity. Black means no record of activity. There is a clear demarcation between corner areas where there is no activity and interior where the flipping is increasingly intense.

Figure 6b., top, shows another boundary condition on the same domain. Each edge is now split in the middle into a segments of extremal tilt ± 1 in an alternating fashion. This choice freezes a lozenge shaped area at each corner (one of which is indicated). Figure 6b., middle, illustrates the cumulative even 1-cycle reversal distribution at equilibrium during the iterates $10^5 - 2 \times 10^5$. In both this and the previous simulation the odd 1-cycles did show an indistinguishable distribution.

In the Kagomé case, too, these are perhaps the simplest boundary conditions yielding non-trivial interiors with symmetries. The bottom row of Figure 6. shows results from a bit smaller run, the cumulative cycle counts from iterates $12 \times 10^3 - 24 \times 10^3$ and $6 \times 10^3 - 12 \times 10^3$ for the two boundary choices (system very close to equilibrium). Here flip activity is rendered dark and the inert background is light grey to make it visible. The coarser appearance is due to the fact that the 1-cycle density is now half of that in the triangular case.

The rendering shows both even 1-triangle and 1-hexagon flips. The darker entries at the center indicate the array of triangles. At the center their flip frequency is about five times that for 1-hexagons. Note that if the arrows were laid down independently and with probability $1/2$ to each orientation on a given edge, the ratio of the flip probabilities of an even 1-triangle to a 1-hexagon would be eight. Our pca here checked the 1-hexagons twice as often as even 1-triangles (with update cycle $\{F_e, F_h, F_o, F_h\}$). Hence if this distribution would be preserved it would generate flip probability ratio exactly four. So we can conclude that the maximally disordered vertex-configurations, the statistics of which we expect to see at the center, are some distance from uniform Bernoulli.

While the fine structure of the interior in Figure 6. depends on the algorithm, the actual arrow distribution at the equilibrium does not. And most importantly the key result, the sharp demarcation of frozen and tempered subdomains akin to the Arctic Circle Theorem is plain in Figure 6.

Due to the corner lozenges (in Figure 6b., top) one can actually compute upper bounds for the entropies on both lattice using the free models much the same way as was done in the square lattice case (e.g. in Figure 6b the upper bound is at most half of those for the free models).

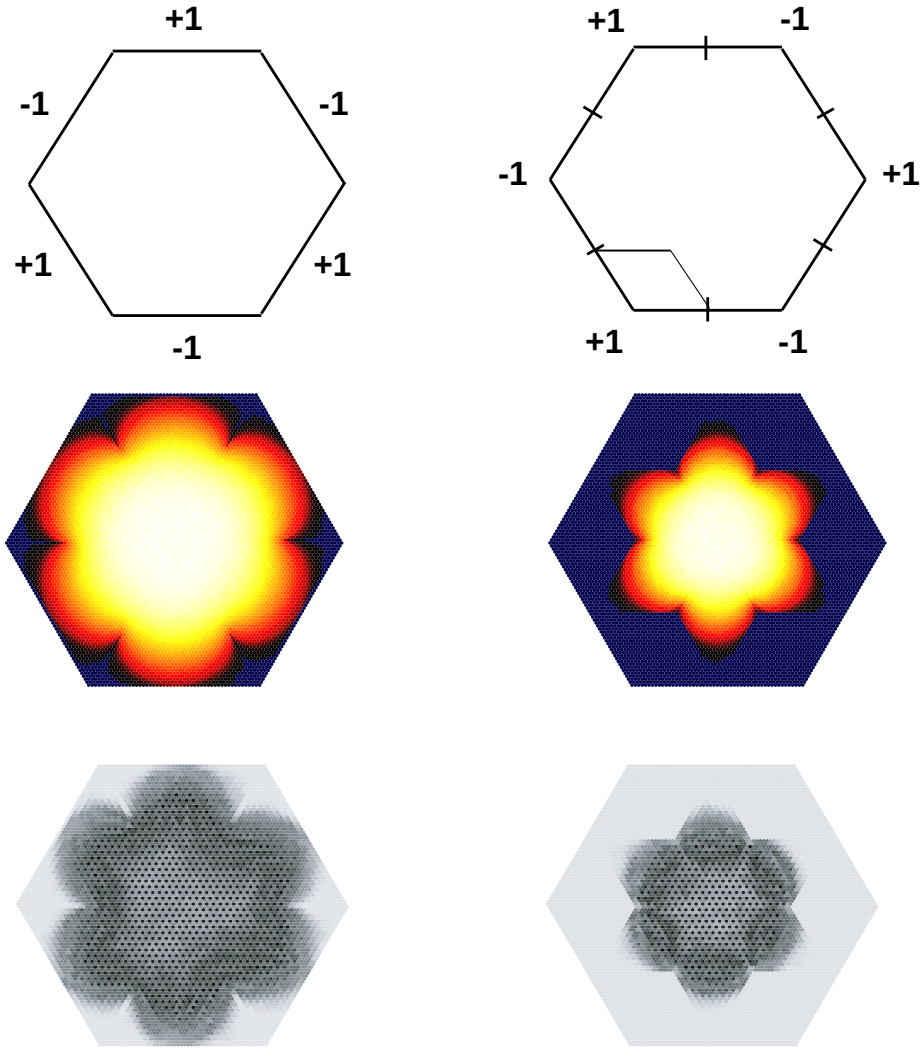

Figure 6a, b (left and right columns). Top row: the domain with boundary signatures, middle row: triangular, bottom row: Kagomé lattice cumulative flip counts. For more data on the runs and renderings, see the text.

4.2. 3.4.6.4. lattice. The Ice on the remaining Archimedean lattice, 3.4.6.4., turns out to be of quite different character. Some unexpected local properties of the lattice overrule the Arctic Phenomena observed above on its kin.

One of these combinatorial oddities already lurks in Figure 2d. The figures attempted to illustrate the maximal boundary tilt in their lower halves. This succeeds for the two other lattices - the heights are indeed a monotone increasing sequences downwards. But for 3.4.6.4. construction like that turns out to be impossible, revealed by the height value 2 at the bottom.

Indeed there are no maximal tilt ± 1 boundary conditions, hence there are no frozen configurations for ice on 3.4.6.4. The absolute value of the tilt is uniformly (in the size of the domain hexagon) bounded away from 1. We conclude the presentation

by formulating a "no-go" Proposition quantifying this and the entropy implications.

The lattice directions of the 3.4.6.4. lattice are the ones it inherits from the underlying triangular lattice $(0, \pm\pi/3)$. Our hexagonal domain has its edges oriented along the lattice directions. Along these edges the 3.4.6.4. lattice viewed as a subset of the triangular lattice has period eight. An arrow block consisting of n consecutive boundary arrows is called an n-**block.**

Proposition 4.3. *Consider a 3.4.6.4. Ice configuration on a N-hexagon and a n-block along any of its straight edges. If the boundary arrows are of period 8 in the n-block the height over the block satisfies $|\Delta h| \leq (3n+7)/4$. For an arbitrary n-block of arrows, $n \geq 15$, the bound is $|\Delta h| \leq (13n+28)/15$. Hence if the boundary height exists in the scaling limit and has tilt, the absolute value of the latter cannot exceed 13/15.*

In any 3.4.6.4. Ice configuration in the set of 1-triangles and 1-lozenges at least 1/7 of them are unidirectional. If the scaling limit entropy for a given boundary exists, it is bounded from below by $\frac{1}{24}\log 2$.

Proof. The first statement follows from the observation that an all-in or all-out 8-block between two neighboring 1-hexagons immediately contradicts the ice rule in one of the boundary vertices. Therefore over such block the absolute height difference is at most 6. If a piece of the edge is made periodically of an 8-block, then in particular the 8-block between two 1-hexagons is an period block. By filling up a n-block with a maximal number of period blocks of length 8 we immediately obtain the first bound.

For the second bound we note that since a 15-block necessarily contains arrows from two 1-hexagons there must be at least one arrow of each orientation in such a block. Hence the height difference cannot exceed 13 in absolute value over the block. The filling argument over the n-block gives the stated bound which in turn implies the scaling limit bound once the tilt exists.

For the latter half of the statement pick a legal configuration and a 1-triangle in it. Suppose that it isn't unidirectional. Up to rotation and reflection it will look like the triangle on the left of Figure 5b. Then either the lozenge on its right is unidirectional or if it isn't, the triangle next to it on the right must be. Hence in any Y-shaped arrangement of 1-triangles and 1-lozenges (as in Figure 5c.) there is at least one 1-cycle. As there are at most 24 arrows in this Y-plaquette determined by the construction, the lower bound follows. □

Recall that besides having completely frozen configurations, by Proposition 4.1. the Ice on triangular and Kagomé lattices can have arbitrarily low entropy configurations (and so can square ice by similar construction). By the Proposition above the situation on 3.4.6.4. differs on both counts and implies that configurations are of quite different character.

The height and entropy bounds of the Proposition are likely not to be tight. Indeed it seems rather difficult to design "stiff" configurations of any kind. The lowest entropy boundary configurations that we have been able to construct have entropy $\frac{1}{6}\log 2$. The seed for such configuration was illustrated in Figure 4d. The fattened hexagon can be extended periodically to an arbitrarily large, unique configuration. In this configuration all the horizontal right leaning parallelograms like the one with bold arrows in the Figure 4d. can generate under the pca action exactly three other local arrow arrangements. Accounting the density of these parallelograms in the configuration immediately gives the entropy value.

The highest entropy boundary condition that we know of (its seed configuration having all 1-cycles directed) has the entropy at least $\frac{1}{4}\log 2$ (which thereby is a lower bound for the entropy of the free model on 3.4.6.4.).

In view of the results it should come as no surprise that the configurations of 3.4.6.4. ice look disordered and rather homogeneous for any boundary condition. Experimenting with hexagons of size around $N = 100$ we found faint traces of boundary dependency in the statistics of the interior (e.g. slight variation in the 1-cycle flip densities). But since frozen states do not exist for 3.4.6.4. there is no possibility of such clear demarcation result as the Arctic Circle/Flower exhibited by the Ice on the other Archimedean lattices.

Acknowledgments. The author thanks L. Markelin for helping with coding and the referee for valuable comments that lead to the improvement of the manuscript.

References

[1] R. J. Baxter, "Exactly Solvable Models In Statistical Mechanics," Academic Press, Inc. [Harcourt Brace Jovanovich, Publishers], London, 1982.
[2] F. Colomo and A. G. Pronko, *The arctic circle revisited*, in "Integrable Systems and Random Matrices," Contemp. Math., **458**, Amer. Math. Soc., Providence, RI, (2008), 361–376.
[3] J. H. Conway and J. C. Lagarias, *Tilings with polyominoes and combinatorial group theory*, J. Combin. Theory Ser. A, **53** (1990), 183–208.
[4] K. Eloranta, *Diamond ice*, J. Stat. Phys., **96** (1999), 1091–1109.
[5] B. Grünbaum and G. C. Shephard, "Tilings And Patterns," W. H. Freeman and Company, New York, 1987.
[6] W. Jockush, J. Propp and P. Shor, "Random Domino Tilings and the Arctic Circle Theorem," arXivmath.CO/9801068.
[7] P. Kasteleyn, *The statistics of the dimer on a lattice, I. The number of dimer arrangements on a quadratic lattice*, Physica, **27** (1961), 1209–1225.
[8] R. Kenyon, *An introduction to the dimer model,*, in "School and Conference on Probability Theory," ICTP Lect. Notes, XVII, Abdus Salam Int. Cent. Theoret. Phys., Trieste, (2004), 267–304 (electronic).
[9] E. Lieb, *Residual entropy of square ice*, Phys. Rev., **162** (1967), 162–172.
[10] J. Propp, "Lattice Structure for Orientation of Graphs," arXivmath.CO/0209005.
[11] W. P. Thurston, *Conway's tiling groups*, Am. Math. Monthly, **97** (1990), 757–773.
[12] P. Walters, "An Introduction To Ergodic Theory," Graduate Texts in Mathematics, **79**, Springer-Verlag, New York-Berlin, 1982.

Received November 2010; revised December 2010.

E-mail address: kari.eloranta@aalto.fi